International Journal of Scientific Research & Engineering Trends
Volume 8, Issue 2, Mar-Apr-2022, ISSN (Online): 2395-566X

A Cycle Simulation Model Of A Diesel Engine For Predicting The Performance Using Python

M.Tech. Scholar Sneha Waghmare, Assistant Prof. B. V. Lande
Department of Mechanical Engineering
Bapurao Deshmukh College of Engineering, Sevagram

Abstract – Experimental research generally requires a significant amount of work, money, and time. To forecast the performance of a diesel engine, a cycle simulation model containing a thermodynamically based single zone combustion model was constructed. For compression ignition (C.I) engines, a thorough computer code was built using 'Python' programming language. Combustion factors including cylinder pressure, heat release, and heat transfer were studied, as well as performance characteristics like work done, braking power, and brake thermal efficiency (BTE). The characteristics at each degree crank angle were computed using the first law of thermodynamics. The maximum pressure and temperature value was determined to be quite near to the experimental value based on the results.

Keywords:CI engine, cycle simulation, numerical model, combustion.

I. INTRODUCTION

Recent developments in the advancement of cleaner diesel engines include the use of common rail systems, fuel injection management methods, exhaust gas recirculation (EGR), exhaust gas after-treatment, and enhanced intake of air, among other things[1]. It's worth noting that the Indian government has pledged to triple bioenergy production in the next ten years, which has fueled the quest for viable biofuels.In order to maintain the global environment and ensure long-term supplies of conventional diesel fuel, it is vital to find alternative fuels that provide engine performance comparable to diesel[2].

Biodiesel, among the alternative fuels, has great promise as an environmentally benign alternative fuel [3]. Due to the food vs. fuel debate, vegetable oil derived from non-edible sources is seen as a possible alternative fuel for compression ignition (CI) engines when contrasted to its edible equivalent. Engine performance was investigated utilising several biodiesel sources[4], including (a) salmon oil [5], (b) rapeseed oil [6–8], (c) rubber seed oil [9], (d) tobacco seed oil [10], (e) sunflower seed oil [11, 12], (f) soybean oil [13], (g) jatrophacurcus oil [14], and (h) karanja oil [15, 16].

Experimentation is usually regarded a vital aspect of development whether creating new engines or enhancing old ones. However, putting the experiment into practice comes with a slew of drawbacks[17]. Preparing the experiment necessitates a significant amount of time and the participation of a larger number of individuals. Furthermore, conducting an experiment entails certain expenses[18, 19]. As a result, more and more technologies are being used to speed up the engine design process while also lowering the cost of the experiment. To begin, the engine cycle is described using several mathematical models. Numerical analyses have been increasingly popular in recent years as a result of advancements in technology. The benefit of numerical analysis is the ability to see the engine cycle, whereas mathematical models just provide numerical numbers. Mechanical calculations are commonly understood to be required when developing any machine assembly. The maximum load values that occur in the observed machine assembly are the most essential when it comes to mechanical calculations. The largest load that occurs during running of an IC engine is a rise in gas pressure in the cylinder [20].

The combustion of diesel fuel is a complicated and diverse process. Thermodynamic and fluid dynamic models are the most common types of combustion models for diesel engines. Thermodynamic models may be divided into three categories: single zone heat release models, phenomenological jet based models, and quasidimensional multi-zone models. Single zone models are good for predicting engine performance because they assume that the cylinder content is homogeneous in composition and temperature. Individual processes in the engine cycle, such as fuel injection, mixture production, heat release, heat transmission, and exhaust generation, are modelled using phenomenological combustion models. Fuel injection, atomization, air entrainment, droplet formation, evaporation, wall impingement, ignition, heat release, and heat transmission are all described using simplified quasi stable equations in quasi-dimensional multi-zone models. Multi-dimensional or computational fluid dynamics (CFD) models are based on solving the governing equations for mass, momentum, and energy conservation, as well as species concentration, using a defined discretization process[21–23].
In their study, Sekmen et al. [24] used numerical simulation to simulate the gasoline IC engine cycle. The

values of the cylinder pressure, temperature, and gas flow speed in the cylinder were observed as simulation output parameters. In their study, Mauro et al. [25] employed two methods to quantify the heat released during combustion. The implementation of the so-called single-zone (SZ) thermodynamic model is the initial technique. It's a mathematical representation. The second method is to use a CFD simulation, which is similar to the one used in this article. They highlighted the fact that the mathematical model takes less time. They also stated that numerical analysis is vastly different from mathematical models[26]. In contrast to these positive aspects of this mathematical model, they claim that the needed input for modelling the heat release is cylinder pressure, which may be acquired empirically or in some other method.The numerical simulation of heat conduction processes in the piston and the modelling of combustion in the cylinder are significant factors in optimising existing engines[27].

Prasad et al. [28] investigated transient heat transfer in a two-dimensional aluminium alloy piston of a semi-adiabatic diesel engine with constant boundary conditions. As a result, the cyclic fluctuations in the heat transfer coefficient and combustion chamber temperature were not taken into consideration. A cycle simulation model is described in this paper. This thermodynamic-based model predicts the performance of a diesel engine running on diesel fuel, working through the engine intake, compression, combustion, expansion, and exhaust processes. For diesel fuel evaluated in this study, the model forecasts the performance of a CI engine in terms of braking power and brake thermal efficiency. The model's inputs include fuel properties, as well as engine design and operational parameters.

1. Computer Program and numerical modelling

The Diesel cycle is used to study the operational characteristics of a single cylinder natural aspirated CI engine, the specifications of which are listed in Table 1. The empirical equations are used in the developed mathematical model to compute the pressure and temperature of cylinder gas, as well as the composition of combustion products. The properties of diesel fuel are as follows; density (831 kg/m^3), calorific value (42.5 MJ/kg).

2.1 Overview

Parameters	Details
Cylinder diameter (D)	87.5 mm
Cylinder number	1
Stroke (S)	110 mm
Connection rod lengths (LB)	234 mm
Intake valve opening	527^0
Intake valve closing	750^0
Exhaust valve opening	340^0
Exhaust valve closing	554^0

For the provided mathematical cycle model, a computerprogramme is created in python environment. The air-fuel combination pulled into the engine cylinder under atmospheric pressure and temperature conditions is replaced with residual gas remaining within the cylinder from the previous cycle, and the pressure and temperature of the previous mixture are modified. The mixture's first thermodynamic characteristics are determined. The clearance volume in a combustion model is assumed to be made up of three regions: "burned region," "burning region," and "unburned area," with compression, combustion, and expansion processes computed using thermodynamic relationships. Thermodynamic equations are used to compute the gas pressure and temperature, as well as the composition of combustion products. Newton Raphson iteration technique is used to solve the equations. After that, values for engine performance such as engine power, specific fuel consumption, mean effective pressure, and thermal efficiency are derived.

1.2 Determination of cylinder volume

At the start, the design parameters such as cylinder size, stroke, compression ratio, connecting rod length, intake and exhaust valve diameters, as well as their opening and closing time values etc. and the operating parameters such as engine speed, universal gas constant, intake air pressure and temperature values, exhaust opposite pressure and temperature, intake and exhaust flow coefficients, specific heat at constant pressure, excess air coefficient, ignition advance, end of combustion point, fuel calorific value, relative humidity and saturation pressure of intake air, atmospheric pressure and temperature, reference pressure and temperature were taken from the data file. The surface area of the piston, the swept volume, and the volume of the combustion chamber were then computed.

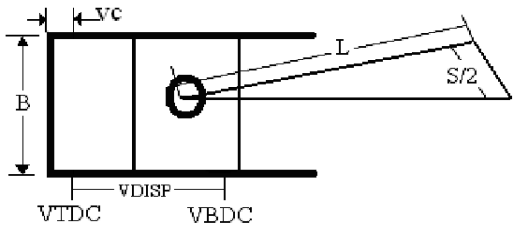

Figure 1: Geometry of reciprocating piston engine

With θ denoting the angular displacement of the crank from BDC, the volume V(θ) at any crank angle is represented by

$$V_\theta = V_{disp} * \left[\frac{r}{r-1} - \frac{1-\cos\theta}{2} + \frac{L}{S} - \frac{1}{2}\sqrt{\left(\frac{2L}{S}\right)^2 - \sin^2\theta}\right] \quad (1)$$

1.3 Determination of Cylinder pressure

The cylinder pressure in a CI engine is determined by the pace at which the fuel burns during combustion. A higher cylinder pressure indicates a faster rate of combustion and heat release.The immediate

pressure inside a cylinder of a diesel engine were measured in this investigation. The gas inside the cylinder was thought to be a perfect gas with physical characteristics that changed with temperature. Other state equations might also be utilised. The following equation can be derived using the equation of state for an ideal gas and the First Law of Thermodynamics:

$$P_\theta = -\gamma \frac{P}{V}\frac{d_v}{d_\theta} + \frac{(\gamma-1)}{V}\frac{dQ}{d_\theta} \quad (2)$$

1.4 Air fuel characteristics

Constant input data and engine constructive properties were read in the application, while O_2, N_2, CO, CO_2, and H_2O properties were read. Variations in pressure and temperature, specific fuel consumption, power output, thermal efficiency, and other factors for16:1 compression ratioare computed and recorded independently in the model. The moles of several species are included in this simulation during the onset of combustion, including O_2, N_2 from intake air and CO_2, N_2 and O_2 from leftover gases. The total combustion equation for a fuel containing C-H-O-N is:

$$C_x H_y O_z + \lambda * y_{cc} * (O_2 + 3.77N_2) \rightarrow xCO_2 + \left(\frac{y}{2}\right) H_2O + (\lambda - 1)y_{cc} * 3.77N_2 \quad (3)$$

The equations were used to compute the total quantity of reactants and products at the commencement of combustion, as well as every degree crank angle.

$$tmr = 1 + \lambda * y_{cc} * 4.773 \quad (4)$$

$$tmp = x + \left({}^{y}/_{4}\right) + 3.773 * \lambda * y_{cc} + (\lambda - 1)y_{cc}$$

1.2 Heat transfer

The heat conduction coefficient was supposed to be a function of engine speed and crank angle, with heat transmission from the combustion chamber to the cooling water temperature being constant. In CI engine, heat transfer is required to keep the cylinder walls, cylinder heads, and piston faces at a safe operating temperature. During every segment of each cycle, heat is transferred from or to the working fluid, and the net work done by the working fluid in one complete cycle is given by.

$$W_{net} = \emptyset \left(p + \frac{\Delta p}{2}\right) * \Delta V \quad (6)$$

Where Δp is the pressure change inside the cylinder as a result of piston motion, combustion, flow into or out of the cylinder and heat transfer. The pressure change Δp due to heat transfer is given by

$$\frac{\Delta p}{p} = \frac{h_c A(T_w - T)}{MC_V T} * \Delta T \quad (7)$$

1.3 Combustion

The mass of the fuel consumed, pressure, and temperature data were determined using the Wiebe function in a subprogram for every 1° of crankshaft revolution. The Wiebe function is a zero-dimensional engine model that has been frequently utilized in engine research, especially for CI applications. In comparison to more sophisticated combustion models, it is a very easy technique to approximate the mass fraction burnt (MFB) during the combustion process.

$$X_b = \left\{1 - exp\left[-a\left(\frac{\theta-\theta_0}{\Delta\theta}\right)^{m+1}\right]\right\} \quad (8)$$

The Wiebe function curve has a distinct S-shaped form and is widely used to describe the combustion process. The mass fraction burnt profile starts at zero, indicating the beginning of combustion, and then rises exponentially to one, marking the conclusion of combustion. The duration of combustion is the difference between those two endpoints.

$$Q = a(m+1)\left(\frac{\theta-\theta_i}{\Delta\theta}\right)^m \exp\left[-a\left(\frac{\theta-\theta_i}{\Delta\theta_c}\right)^{m+1}\right] \quad (9)$$

The above equation can be expressed in terms of KJ/^{0}CA as follows;

$$\frac{dQ_c}{d_\theta} = a(m+1)\left(\frac{Q_{av}}{\Delta\theta_c}\right)^m exp\left[-a\left(\frac{\theta-\theta_i}{\Delta\theta_c}\right)^{m+1}\right] \quad (10)$$

1.4 Frictionallosses

Frictional losses have a direct impact on maximum brake torque and minimum brake specific fuel consumption, and are frequently used as a criterion for engine design. These losses affect not just the power but also the size of the cooling systems. The following empirical relations are used to compute the mean effective losses of power due to friction in various moving components.

1.4.1 Mean effective pressure (MEP) lost to overcome friction due to gas pressure behind the rings.

$$F_{mep\,1} = 0.42 * (p_a - p_{imf}) * {}^{S}/_{B^2} * \left(0.0888C_r + 0.182\,Cr1.33{-}0.394Cm100{*}10\right) \quad (11)$$

1.4.2 Mean effective pressure absorbed in friction due to wall tension of rings

$$F_{mep\,2} = 10 * \frac{0.377\,Sn_{pr}}{b^2} \quad (12)$$

1.4.3 MEP absorbed in friction due to piston and rings

$$F_{mep\,3} = 12.85 * \frac{P_{sl}}{BS} * \frac{100\,C_m}{1000} \quad (13)$$

1.4.4 Blow by loss

$$F_{mep\,4=\sqrt{P_a - P_{imf}}} * \left[0.212\,r^4 - (0.034 + 0.0001055r) * N10001.18\right] \quad (14)$$

1.4.5 MEP lost in overcoming inlet and throttling losses

$$F_{mep\,5} = {}^{P_e}/_{2.75} + P_{imf} \quad (15)$$

1.4.6 MEP absorbed to overcome friction due to the valve gear

$$F_{mep\,6} = 0.226 * \left(30 - {}^{4N}/_{1000}\right) * {}^{GH^{1.75}}/_{B^2S}$$ (16)

1.4.7 MEP lost in pumping

$$F_{mep\,7} = 0.0275 * \left({}^{N}/_{1000}\right)^{1.5}$$ (17)

1.4.8 MEP absorbed in bearing friction

$$F_{mep\,8} = 0.0564 * {}^{B}/_{S} * {}^{N}/_{1000}$$ (18)

1.4.9 MEP absorbed in overcoming the combustion chamber and wall pumping losses

$$F_{mep\,9} = \sqrt{{}^{P_{imep}}/_{11.45}} * 0.0915\left({}^{N}/_{1000}\right)^{1.7}$$ (19)

Total MEP lost in friction

$$F_{mep} = F_{mep\,1} + \ldots\ldots\ldots\ldots\ldots\ldots + F_{mep\,9}$$ (20)

The net work done during the cycle, and thus the indicated mean effective pressure, can be used to determine the indicated power. The difference between the displayed mean effective pressure and the frictional mean effective pressure is the brake mean effective pressure. As a result, it determines brake power based on known brake mean effective pressure, stroke volume, and speed.

2. Result and discussion

The Combustion characteristics such as cylinder pressure, heat release rate, ignition delay, and combustion zone temperature are explored in this study.

3.1 Cylinder volume wrt crank angle

The cylinder volume is calculated with the help of developed program and plotted against the crank angle. Figure 2 shows the variation of cylinder volume with respect to crank angle. The cylinder volume is maximum at 0^0, 360^0 and 720^0 as the piston is at the bottom dead center. The cylinder volume is minimum at 180^0 and 540^0 as the piston is located at the top dead center of the cylinder.

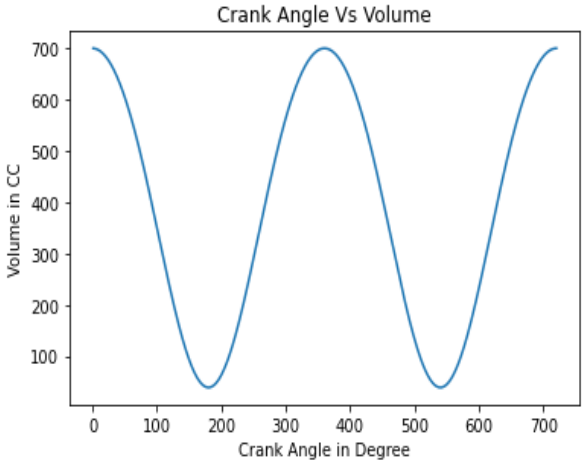

Figure 2: Volume of cylinder wrt crank angle.

2.2 Variation of pressure during compression stroke

Figure 3 shows pressure inside the cylinder during compression with respect to crack angle. The compression stroke is assumed to be start at 0^0 and ended at 153^0. The maximum pressure attained during the compression stroke was 22.43 bar.

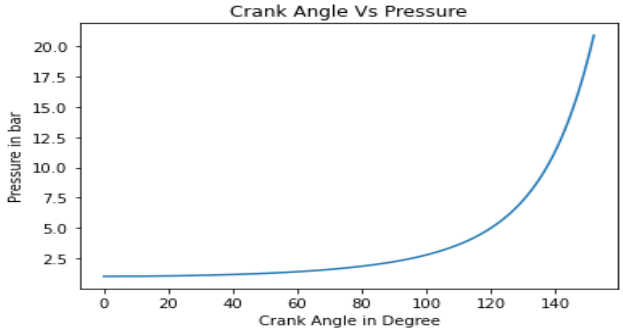

Figure 3: Variation of temperature during compression stroke

2.3 Variation of pressure during delay period

Figure 5 shows the variation of pressure inside the cylinder during the delay period. The delay period is assumed to be between 153^0 to 175^o. The pressure inside the cylinder at the beginning and end of the delay period was 22 bar and 55 bar respectively.

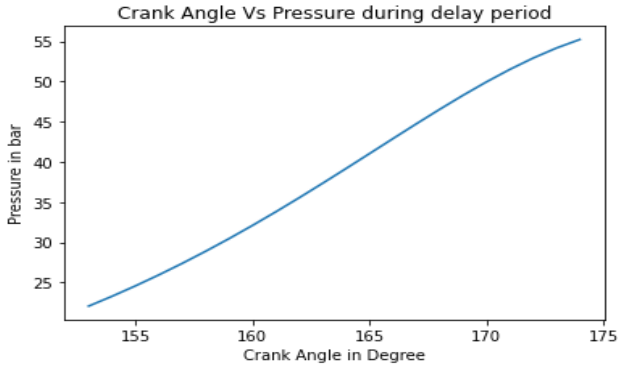

Figure 4: Pressure inside the cylinder during delay period

2.4 Variation of temperature during delay period

Figure 6 shows the graph between the temperatures inside the cylinder during delay period with respect to crank angle. As discussed earlier the delay period starts from 153^0 and ends at 175^0. The temperature at the beginning of the delay period predicted by the model is 714 ^{0}C while at the end 938 ^{0}C.

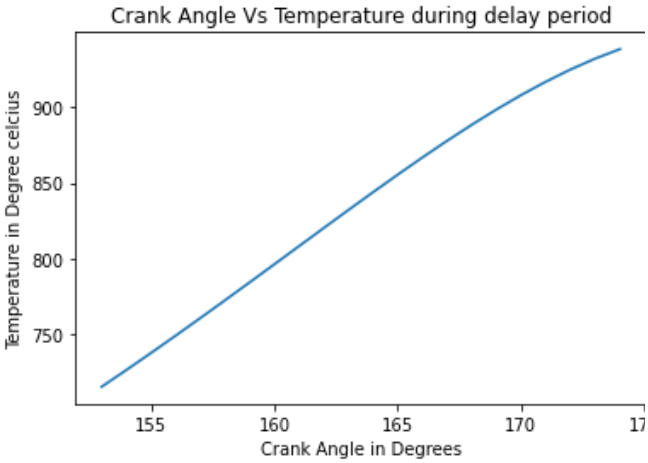

Figure 5: Temperature inside the cylinder during delay period

2.5 Variation of temperature variation during combustion stroke

Figure 7 shows the variation of temperature during the combustion period. The combustion starts at 175^0 just before the end of compression stroke and ends at 225^0. As shown in figure 7 the temperature predicted by the model at the start and end of the combustion is 1191 ^{0}C and 2540 ^{0}C respectively. The sudden rise in temperature was observed at the start of the combustion period.

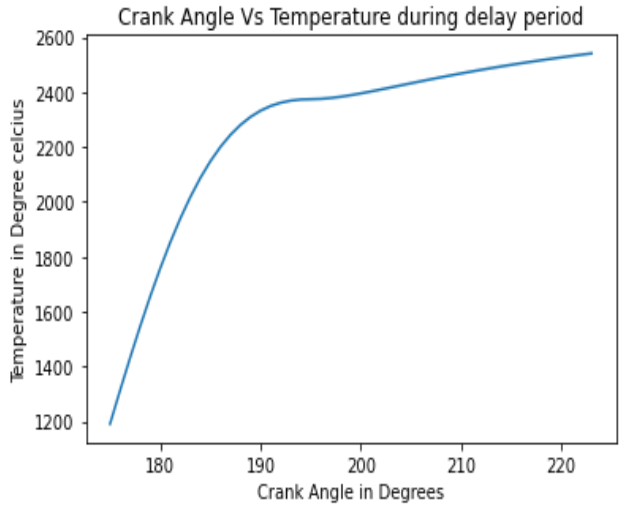

Figure 6: Temperature variation during combustion

2.6 Variation of pressure during combustion stroke

Figure 8 shows the variation of pressure during the combustion period. The process of combustion as stated earlier starts from 175^0 and ends at 225^0. The maximum pressure is attained at the beginning of combustion and then pressure gradually lowers as the piston moves from top dead center to bottom dead center.

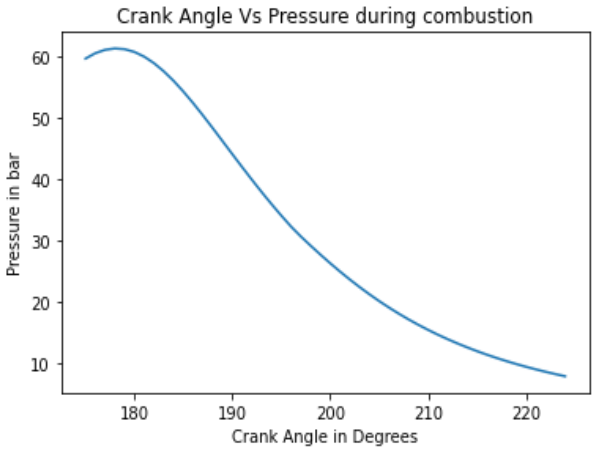

Figure 7: Variation of pressure during combustion period

2.7 Variation of pressure during expansion stroke

Figure 9 shows the variation of pressure inside the cylinder during the expansion stroke. The expansion stroke starts at 225^0 and ends at 360^0. The pressure inside the cylinder at the beginning of the expansion stroke predicted by the model is 7.56 bar while at the end of expansion stroke is 0.99 bar.

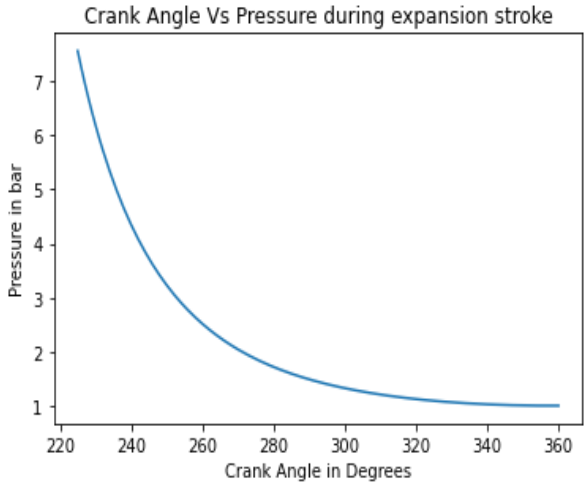

Figure 8: Pressure inside the cylinder during expansion stroke

2.8 Variation of temperature during expansion stroke

Figure 10 shows the variation of temperature during expansion stroke. The expansion stroke starts from 225^0 and ends at 360^0. The developed model shows highest temperature at the start of expansion stroke and lowest pressure at the end of expansion stroke. The model predicted 2540 ^{0}C at the start of expansion stroke while 1718 ^{0}C at the end of an expansion stroke.

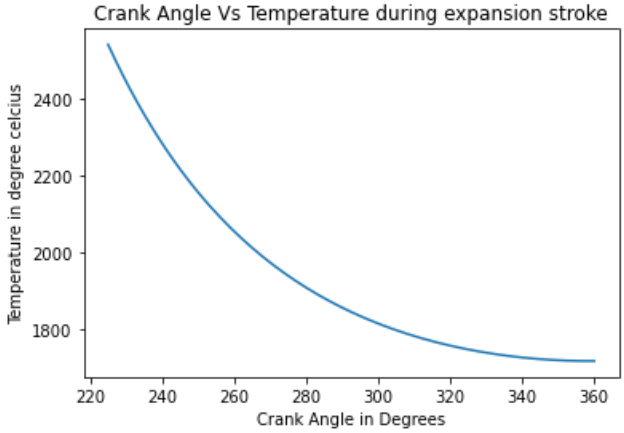

Figure 9: Variation of temperature during expansion stroke.

2.9 Frictional losses

The frictional losses predicted by the model are presented in table 2.

Table 1: Frictional losses predicted by model

Frictional loss	Quantity in bar
Friction due to gas pressure behind the rings	0.2181
Friction due to wall tension of rings	0.1624
Friction due to piston and ring friction	0.4951
Blow-by loss	0.069
Inlet and throttle loss	1.363
Friction due to valve gear	0.000018
Pumping Loss	0.050
Bearing Friction	0.067
Friction due to gas pressure behind the rings	0.2181

The other parameters such as compression, combustion, expansion work and thermal, mechanical and brake thermal efficiency predicted by the model are given in table 3.

Table 2: Parameters predicted by model

Parameters	Quantity
Indicated power	12.2 kW
Compression work	388.37 J
Combustion work	-375.42 J
Expansion work	988.95 J
Net work	976 J
Thermal efficiency	42.35
Brake mean effective pressure	11.92 bar
Brake power	9.98 kW
Mechanical efficiency	81.87
Brake thermal efficiency	34.68

III.CONCLUSION

The performance of a single cylinder four stroke diesel engine fueled by diesel is predicted using a diesel engine cycle simulation model. The simulation of CI engine for the diesel fuel is done in python environment. The following conclusions can be drawn from the study.

1. Computer simulation can be an effective method to predict the performance of CI engine.
2. Once the model is developed, the same model can be used for various fuels and its blends to predict its performance.
3. The maximum pressure predicted by the model is 61.25 bar and it occurred during the combustion stroke of the engine.
4. The maximum temperature predicted by the model is 2540 ^{0}C and it also occurred during the combustion stroke of the engine.

No study is without limitations, the model developed have to be validated with the experimental results. The authors are planning to validate the developed model with experimental data in their further study.

REFERENCES

[1] Rakopoulos, C. D.; Antonopoulos, K. A.; Rakopoulos, D. C.; Hountalas, D. T. Multi-Zone Modeling of Combustion and Emissions Formation in DI Diesel Engine Operating on Ethanol-Diesel Fuel Blends. Energy Convers. Manag., **2008**, 49 (4), 625–643. https://doi.org/10.1016/j.enconman.2007.07.035.

[2] Canakci, M.; Sayin, C.; Ozsezen, A. N.; Turkcan, A. Effect of Injection Pressure on the Combustion, Performance, and Emission Characteristics of a Diesel Engine Fueled with Methanol-Blended Diesel Fuel. Energy & Fuels, **2009**, 23 (6), 2908–2920. https://doi.org/10.1021/ef900060s.

[3] Carraretto, C.; Macor, A.; Mirandola, A.; Stoppato, A.; Tonon, S. Biodiesel as Alternative Fuel: Experimental Analysis and Energetic Evaluations. Energy, **2004**, 29 (12), 2195–2211. https://doi.org/https://doi.org/10.1016/j.energy.2004.03.042.

[4] Raut, L. P. Computer Simulation of CI Engine for Diesel and Biodiesel Blends. Int. J. Innov. Technol. Explor. Eng., **2013**, No. 32, 2278–3075.

[5] Reyes, J. F.; Sepúlveda, M. A. PM-10 Emissions and Power of a Diesel Engine Fueled with Crude and Refined Biodiesel from Salmon Oil. Fuel, **2006**, 85 (12), 1714–1719. https://doi.org/https://doi.org/10.1016/j.fuel.2006.02.001.

[6] Labeckas, G.; Slavinskas, S. The Effect of Rapeseed Oil Methyl Ester on Direct Injection Diesel Engine Performance and Exhaust Emissions. Energy Convers. Manag., **2006**, 47 (13), 1954–1967. https://doi.org/https://doi.org/10.1016/j.enconman.2005.09.003.

[7] Tsolakis, A.; Megaritis, A.; Wyszynski, M. L.; Theinnoi, K. Engine Performance and Emissions of a Diesel Engine Operating on Diesel-RME (Rapeseed Methyl Ester) Blends with EGR (Exhaust Gas Recirculation). Energy, **2007**, 32 (11), 2072–2080. https://doi.org/https://doi.org/10.1016/j.energy.2007.05.016.

[8] Raut, L. P.; Taiwade, R. V. Wire Arc Additive Manufacturing: A Comprehensive Review and Research Directions. J. Mater. Eng. Perform., **2021**, 30 (7), 4768–4791. https://doi.org/10.1007/s11665-021-05871-5.

[9] Ramadhas, A. S.; Muraleedharan, C.; Jayaraj, S. Performance and Emission Evaluation of a Diesel Engine Fueled with Methyl Esters of Rubber Seed Oil. Renew. Energy, **2005**, 30 (12), 1789–1800. https://doi.org/https://doi.org/10.1016/j.renene.2005.01.009.

[10] Usta, N. An Experimental Study on Performance and Exhaust Emissions of a Diesel Engine Fuelled with Tobacco Seed Oil Methyl Ester. Energy Convers. Manag., **2005**, 46 (15), 2373–2386. https://doi.org/https://doi.org/10.1016/j.enconman.2004.12.002.

[11] Neto da Silva, F.; Salgado Prata, A.; Rocha Teixeira, J. Technical Feasibility Assessment of Oleic Sunflower Methyl Ester Utilisation in Diesel Bus Engines. Energy Convers. Manag., **2003**, 44 (18), 2857–2878. https://doi.org/https://doi.org/10.1016/S0196-8904(03)00067-0.

[12] Raut, L. P.; Taiwade, R. V. Microstructure and Mechanical Properties of Wire Arc Additively Manufactured Bimetallic Structure of Austenitic Stainless Steel and Low Carbon Steel. J. Mater. Eng. Perform., **2022**. https://doi.org/10.1007/s11665-022-06856-8.

[13] Hu, Z.; Tan, P.; Yan, X.; Lou, D. Life Cycle Energy, Environment and Economic Assessment of Soybean-Based Biodiesel as an Alternative Automotive Fuel in China. Energy, **2008**, 33 (11), 1654–1658. https://doi.org/https://doi.org/10.1016/j.energy.2008.06.004.

[14] Lakshmi Narayana Rao, G.; Durga Prasad, B.; Sampath, S.; Rajagopal, K. Combustion Analysis of Diesel Engine Fueled with Jatropha Oil Methyl Ester - Diesel Blends. Int. J. Green Energy, **2007**, 4 (6), 645–658. https://doi.org/10.1080/15435070701665446.

[15] Raheman, H.; Phadatare, A. G. Diesel Engine Emissions and Performance from Blends of Karanja Methyl Ester and Diesel. Biomass and Bioenergy, **2004**, 27 (4), 393–397. https://doi.org/https://doi.org/10.1016/j.biombioe.2004.03.002.

[16] Panigrahi, N.; Mohanty, M. K.; Acharya, S. K.; Mishra, S. R.; Mohanty, R. C. Experimental Investigation of Karanja Oil as a Fuel for Diesel Engine-Using Shell and Tube Heat Exchanger. **2014**, 8 (1), 89–96.

[17] Patil, N. A.; Raut, L. P. VIBRATION ANALYSIS OF CI ENGINE USING FFT ANALYZER. Int. J. Res. Eng. Technol., **2005**, 5 (1), 293–298.

[18] Kale, R. P.; Raut, L. P.; Talmale, P. Kaizen & Its Applications – A Japanese Terminology Referred to Continuous Improvement. Int. J. Sci. Res. Dev., **2015**, 3 (02), 1772–1775.

[19] Bhoyar, A. S.; Raut, L. P.; Mane, S. Total Productive Maintenance : The Evolution in Maintenance and Efficiency Total Productive Maintenance : The Evolution in Maintenance and Efficiency. Int. J. Eng. Res. Appl., **2017**. https://doi.org/10.9790/9622-0711012632.

[20] Grujic, I.; Stojanovic, N.; Pesic, R. MVM2018-062 NUMERICAL MODELING OF IC ENGINE COMBUSTION PROCESS. **2018**, No. October.

[21] Ramadhas, A. S.; Jayaraj, S.; Muraleedharan, C. Theoretical Modeling and Experimental Studies on Biodiesel-Fueled Engine. Renew. Energy, **2006**, 31 (11), 1813–1826. https://doi.org/https://doi.org/10.1016/j.renene.2005.09.011.

[22] Tawele, P.; Shinde, G.; Raut, L. Design and Development of 3-Way Dropping Dumper. Int. J. Emerg. Technol. Adv. Eng., **2014**, 4 (9), 766–775.

[23] Raut, L. P.; Jaiswal, S. B.; Mohite, N. Y. Design, Development and Fabrication of Agricultural Pesticides Sprayer with Weeder. Int. J. Appl. Res. Stud., **2013**, 2 (11), 2278–9480.

[24] Sekmen, P.; Sekmen, Y. Mathematical Modeling of a SI Engine Cycle with Actual Air-Fuel Cycle Analyses. Math. Comput. Appl., **2007**, 12 (3), 161–171. https://doi.org/10.3390/mca12030161.

[25] Mauro, S.; Şener, R.; Gül, M. Z.; Lanzafame, R.; Messina, M.; Brusca, S. Internal Combustion Engine Heat Release Calculation Using Single-Zone and CFD 3D Numerical Models. Int. J. Energy Environ. Eng., **2018**, 9 (2), 215–226. https://doi.org/10.1007/s40095-018-0265-9.

[26] Gayatri D. Barai, L. R. Performance Analysis of IC Engine Using Air Energizer. Int. J. Res. Eng. Technol., **2015**, 04 (04), 774–778. https://doi.org/10.15623/ijret.2015.0404135.

[27] Raut, L. P.; Dhandare, V.; Jain, P.; Ghike, V.; Mishra, V. Design, Development and Fabrication of a Compact Harvester. IJSRD -International J. Sci. Res. Dev., **2014**, 2 (10), 2321–2613.

[28] Prasad, R.; Samria, N. K. Transient Heat Transfer Analysis in an Internal Combustion Engine Piston. Comput. Struct., **1990**, 34 (5), 787–793. https://doi.org/https://doi.org/10.1016/0045-7949(90)90146-S.